# Removal of guaifenesin and amprolium drugs from wastewater using ecofriendly low-cost biopolymer: adsorption isotherms, kinetics models and thermodynamic studies

Amr Mohamed[a,b,*], Hanaa A. Hassanin[c], Samah Ali[a,d,*]

[a]*Chemistry Department, College of Science, Taibah University, Al-Madinah Al-Munawarah, Saudi Arabia,*
*emails: addeck@taibahu.edu.sa (A. Mohamed), samali@taibahu.edu.sa (S. Ali)*
[b]*The Higher Institute of Optics Technology (HIOT), Heliopolis 17361, Cairo, Egypt*
[c]*Department of Chemistry, Faculty of Science, Ain Shams University, 11566 Abbassia, Cairo, Egypt,*
*email: hanaaeisa@sci.asu.edu.eg (H.A. Hassanin)*
[d]*The National Organization for Drug Control and Research, Giza, Egypt*

## ABSTRACT

An environmentally safe, economic, yet simple approach was presented in this study for the removal of the traces of guaifenesin (GUA) and amprolium (AMP) drugs from wastewater using chitosan (CS) biopolymer. The removal capacity was investigated under several variables including pH, contact time, adsorbent dose, and drug capacity. The study of adsorption isotherm models demonstrates that Langmuir model is more likely to illustrate the adsorption process more than Freundlich with correlation coefficient ($R^2$) of 0.984 and 0.994 with ($q_m$) of 2.78 and 1.33 for both GUA and AMP, respectively. Four kinetic models were assessed for the adsorption process. The results indicate that the adsorption system follows the pseudo-second-order model which was confirmed by its higher correlation coefficient ($R^2 \approx 0.99$) for both GUA and AMP, suggesting that chemical adsorption is the rate-limiting step of the adsorption mechanism. Thermodynamic studies were carried out to determine $\Delta H°$, $\Delta G°$, $\Delta S°$. The positive values of $\Delta H°$ and $\Delta G°$ indicated that the sorption of both drugs onto CS is an endothermic nonspontaneous and the system gained energy from an external source.

*Keywords:* Guaifenesin; Amprolium; Chitosan biopolymer; Wastewater treatment

## 1. Introduction

The treatment of wastewater from pollutants such as pharmaceuticals and personal care products (PPCPs) is a major challenge for many countries around the world to meet the growing need for agricultural and industrial development. Pharmaceutical compounds have been detected in environmental samples with concentration levels ranging between ng/L to mg/L [1]. It is known that the prolonged exposure to antibiotics residues in water makes them inactive or less effective, in addition to the severe health issues for both humans and animals [2–4]. Guaifenesin (GUA) [3-(2-methoxyphenoxy)-1,2-propanediol], is a pharmaceutical compound used for the treatment of cough, asthma, gout, muscle relaxant and rhinitis [5,6]. GUA has a high solubility in water, and therefore, its presence in water and wastewater is highly probable [7]. Amprolium (AMP) [5-(2-methylpyridin-1-ium-1-yl) methyl-2-propyl-pyrimidin-4-amine chloride] is a veterinary drug used for farm animals [8]. It is used for the prevention

* Corresponding authors.

of coccidiosis that specially affects poultry, which is able to outbreak through the whole population of the field in a short period of time in case of the absence of control [9,10]. Therefore, poultry should be routinely given food containing the amprolium drug to prevent the spread out of this disease. For this reason, amprolium residues can commonly be detected in poultry products [11].

Residual veterinary drugs and pharmaceutical compounds (PCs) in wastewater, surface water and soil environments may facilitate the spread of antibiotics-resistant bacteria and eventually impair the clinical or veterinary efficacy of antibiotics [12–14]. These compounds are increasingly detected in wastewater in large quantities because of the population growth, the health development, agricultural and industrial activities. Therefore, various techniques were developed for the treatment and removal of (PCs) from wastewater. These techniques include chemical methods such as advanced oxidation processes (Fenton reagent, ozonation), physical methods such as ion exchange and adsorption, and biological methods like aerobic degradation and electrocoagulation [15–20].

Adsorption is one of the most extensively used approaches for wastewater treatment from organic and inorganic pollutants, it has several advantages over the other methods like its low cost, simple design, availability of adsorbents, high efficiency and reusability [21]. There are two types of adsorbents, natural adsorbents and synthetic adsorbents. Synthetic adsorbents are widely used as polymeric media to extract pollutants from wastewater due to its high adsorption capacity, chemical stability and strength [22]. Natural adsorbents include clays, charcoal, zeolites, sawdust, straw, clay minerals, rice husk, bark, and cotton waste [23–27]. These natural adsorbents are commonly cheap, available, have a good sorption property, able to remove pollutants with short contact period, simple to design, easy to operate and can handle pollutants without generating toxic by-products.

Chitosan (CS) is the most dominant biopolymer in nature after cellulose. It was found to be one of the most effective materials for adsorption applications. it is used to adsorb dyes, metal complexes, metal ions, phenols, and drugs and it has the advantage of higher antibacterial activity and lower toxicity [28–31].

This work aims to investigate the suitability and effectiveness of a cheap environmental-friendly sorbent material for the removal of guaifenesin (GUA) and amprolium (AMP) drug traces from aqueous media for possible application in environmental remediation of polluted water bodies. The natural biosorbent chitosan (CS) was tested for the removal of both guaifenesin (GUA) and amprolium (AMP) drugs from aqueous media. Several parameters were studied to investigate the ability of (CS) for removing these drugs from wastewater including pH, temperature, shaking time, adsorbent mass, and drug capacity. The adsorption isotherm models, kinetic models as well as thermodynamic studies were carried out for the removal of both drugs using chitosan.

## 2. Experimental set-up

### 2.1. Materials

Guaifenesin drug (GUA) was purchased from TCI (Tokyo Chemical Industry Co., Ltd.) and amprolium (AMP) drug was provided by NODCAR (The National Organization for Drug Control and Research, Egypt). Both drugs were prepared in solutions of 100 ppm for further study. Chitosan (CS) ($d$ = 0.15 g/mL, moisture content = 8.2%) was purchased from Sigma-Aldrich (St. Louis, MO, USA). The applied chitosan had a deacetylation degree of 70%–85%.

### 2.2. Instrumentation

The pH of working solutions was measured using a pH meter (HANNA-Instruments HI 2211, Italy) that was calibrated against a standard buffer. An automated shaker (Stuart orbital shaker I SSL1 I) was used to equilibrate adsorption experiments. Spectrophotometric measurements were done on UV-Vis spectrophotometer (Thrmoscientific Genesys 10S). The surface functional groups of modified chitosan were confirmed using Fourier-transform infrared spectrometer (FTIR) (FTIR-8400S Shimadzu), scanning electron microscopy (SEM) (Joel, 1400, Japan).

### 2.3. Methods

For the preparation of stock solutions, 0.01 g of each drug was completely dissolved in 10 mL measuring flask with distilled water to reach the concentration of 100 ppm. For the construction of the calibration curves, a series of standard solutions (5.0–60 ppm) were made by appropriate dilution. The absorbance of each standard solution was measured at $\lambda_{max}$ = 275 nm and $\lambda_{max}$ = 265 nm for GUA and AMP drugs, respectively.

### 2.4. Adsorption study

Batch equilibrium methods were used to study the adsorption process at room temperature. The required concentrations of both drugs were obtained by appropriate dilution of stock solution (100 ppm). Batch experiments were conducted by placing variable amounts of chitosan in a 10 mL Erlenmeyer flask with adequate volumes of aqueous solution of drugs (10 ppm). The mixture was agitated at constant speed of 200 rpm by an automated shaker. The remaining drug concentration was measured spectrophotometrically. The pH effect on the uptake of drugs was determined in pH range of (4.5–8.0) using 0.02 g of chitosan and 10 ppm of the drug solution, then the solution was shaken for 30 min to maintain equilibrium. To attain the desired pH, acetate and phosphate buffer was used. To assess the effect of shaking time on the adsorption process, 0.02 g of chitosan was introduced to 5 mL of each drug (10 ppm) at pH of 5.0 with shaking at different time intervals (0–120 min). For studying the influence of temperature from (25°C–80°C), 0.02 g of chitosan was added to 5 mL of each drug (10 ppm) solution at pH of 5.0 and shaking for 30 min. To test the effect of sorbent amount on the removal of drugs, different amounts of chitosan (0.02–0.2 g) were added to the drug solutions (10 ppm) at pH of 5.0 and shaking time of 30 min. The effects of initial drugs concentration on adsorption were studied in the range from 10 to 100 ppm at pH 5.0 for 30 min. The drugs concentration in the remaining solution was estimated spectrophotometrically. Eq. (1) was used to calculate the removal percentage of the adsorbed drug:

$$\%R = \frac{(C_0 - C_e)}{C_0} \times 100 \tag{1}$$

where $C_0$ and $C_e$ represent initial and final concentrations of the drug, respectively. The quantity of adsorbed particles per 1 g of adsorbent ($q_e$) is determined using Eq. (2):

$$q_e = \frac{(C_0 - C_e)V}{m} \tag{2}$$

where $V$ and $m$ are the volume used in liters and the mass of chitosan in grams, respectively.

## 3. Results and discussions

### 3.1. Characterization

#### 3.1.1. Morphological characterization by SEM

The morphology of the CS before and after the adsorption of both GUA and AMP drugs was examined by SEM as shown in Fig. 1. Chitosan exhibited a rough nonporous, smooth membranous phase consisting of micro-fibrils, orifices dome shaped [32,33] and smooth surfaces provide a high area for the adsorption. After adsorption, the GUA and AMP adhered to the surface of chitosan, this is shown as white areas in SEM images. The surface of the CS became denser and rougher after adsorption of GUA and AMP, which contain functional groups that control the adsorption process [34]. The surface area of CS sorbent was measured by Brunauer–Emmett–Teller and was found to be 2 $m^2$/g. These values are matching with the SEM images.

#### 3.1.2. Fourier transform-infrared spectroscopic analysis

FTIR spectroscopy was used to identify the characteristic vibrational modes for chitosan and to confirm the successful adsorption of both drugs onto its surface. Fig. 2 represents the FTIR spectra for chitosan before and after the adsorption of GUA and AMP. The FTIR spectrum for pristine chitosan Fig. 2a shows a broad band at 3,440 $cm^{-1}$, which is attributed to O–H/N–H groups. The peaks that appear in the range of 2,870–2,920 $cm^{-1}$ are related to $CH_2$/$CH_3$ groups. The bands at 1,656 and 1,557 $cm^{-1}$ are assigned to amide I and amino groups, respectively. In addition, the bands at 1,376; 1,060 and 600 $cm^{-1}$ refer to vibrational modes of C–N,

C–O, and C–H of aromatic rings, respectively [35,36]. Fig. 2b and c show the FTIR spectrum of chitosan after adsorption of AMP and GUA, respectively. It can be clearly seen that there are significant changes in the infrared spectrum of chitosan after adsorption of both drugs such as the band at 3,440 $cm^{-1}$ that is shifted to 3,430 and 3,311 $cm^{-1}$ for AMP and GUA, respectively. Furthermore, the peaks at 1,656; 1,557; 1,060 and 600 $cm^{-1}$ are slightly shifted and/or decreased in intensity after the adsorption of both drugs which confirms the interaction with chitosan [35,37]. The FTIR spectra of the parent drugs were examined to further confirm the interaction between both drugs and chitosan. Fig. 2d shows the FTIR of (AMP) it shows a small broad peak at 3,200 $cm^{-1}$ related to N–H stretches for primary amine. The characteristic bands at 2,999; 2,625; 1,680 and 1,270 $cm^{-1}$ for C–H ($sp^3$) vibration, quaternary ammonium salt, C=C of the benzene ring, and C–N stretch, respectively [38]. FTIR spectrum of GUA is shown in Fig. 2e and it consists of the characteristic peaks at 3,448; 3,111 and 1,730 $cm^{-1}$ and the peaks in the range 1,250–860 $cm^{-1}$ correspond to O–H, C–H stretching, C=O, and C–H bending, respectively [39].

It can be observed that there are significant changes on the FTIR spectra of GUA and AMP after adsorption by chitosan confirming the interaction between both drugs
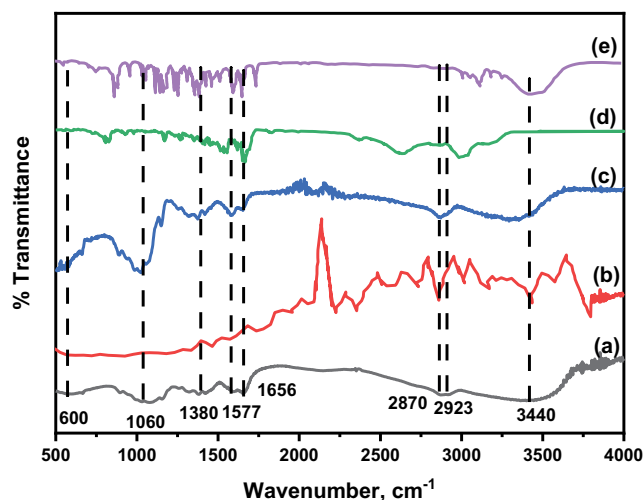
Fig. 2. Fourier-transform infrared spectra for (a) chitosan, (b) chitosan after adsorption of amprolium, and (c) chitosan after adsorption of guaifenesin, (d) amprolium, (e) guaifenesin.
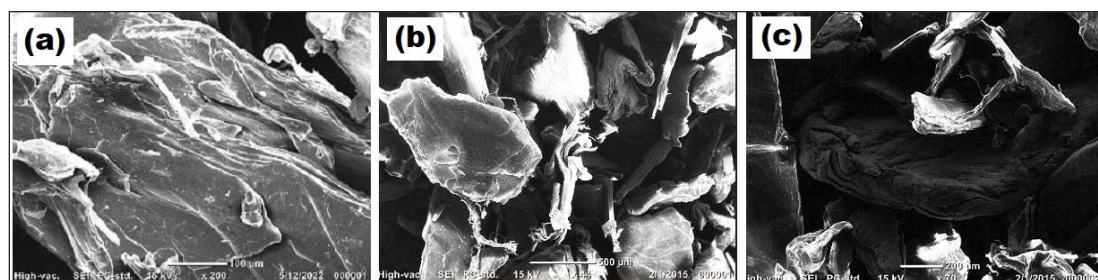
Fig. 1. Scanning electron microscopy images of: (a) chitosan, (b) chitosan after adsorption of amprolium, and (c) chitosan after adsorption of guaifenesin.

and chitosan. The suggested mechanism of adsorption is shown in Fig. 3.

### 3.2. Effect of pH

The effect of pH on the removal of both drugs by CS was investigated within a pH range of 4.5–8.0. Fig. 4a shows pH effect on the upta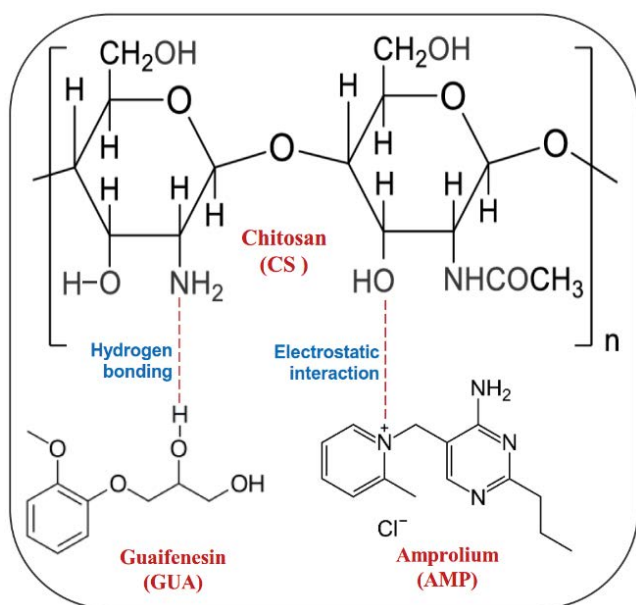ke of GUA and AMP. It can be seen that pH has almost no influence on the uptake of GUA with percentage removal of approximately 52% since the $pK_a$ for GUA is 13.62, which means that it is neutral over a wide range of pH [41]. However, the removal of AMP increases from pH 4.5–6.0 to reach its maximum at pH 6.0 to be 26% then remains constant from pH 6.0–8.0. AMP has two charged groups within its structure. The first one is $(NH_4^+)$ group that is pH independent, whereas the second amino which is located in the pyrimidine ring has $pK_a$ value of 5.3. At lower pH, AMP molecule is doubly charged $(AMP^{++})$ which in turn increases the electrostatic repulsion effect between protonate chitosan (zero-point charge to 6.8) [35], while at higher pH, the adsorption uptake slightly increased as a consequence of the decrease in the charge of the AMP molecule which is almost singly charged $AMP^+$ [42]. Furthermore, the ammonium group of AMP can be coordinated to the hydroxyl group of chitosan [43]. Accordingly, pH 6.0 was selected for all subsequent measurements of GUA and AMP drugs.

### 3.3. Effect of shaking time

Fig. 4b shows the effect of shaking time on the uptake of GUA and AMP drugs. The effect of shaking time was studied at time intervals between 0 to 120 min. The maximum removal percentage for GUA and AMP after a period of 60 min was found to be 95% and 79%, respectively. The percentage of GUA adsorption has increased from 47.3% to 91.7% after 60 min while that of AMP has increased from 66.7% to 78.3% after 45 min, after which, no further increase was observed, probably due to the decrease in the number of available free sites. For this reason, 60 min was considered as the best sorbent exposure time for both drugs.



Fig. 3. Chemical structure of chitosan sorbent, guaifenesin and amprolium drugs with the suggested adsorption mechanism.
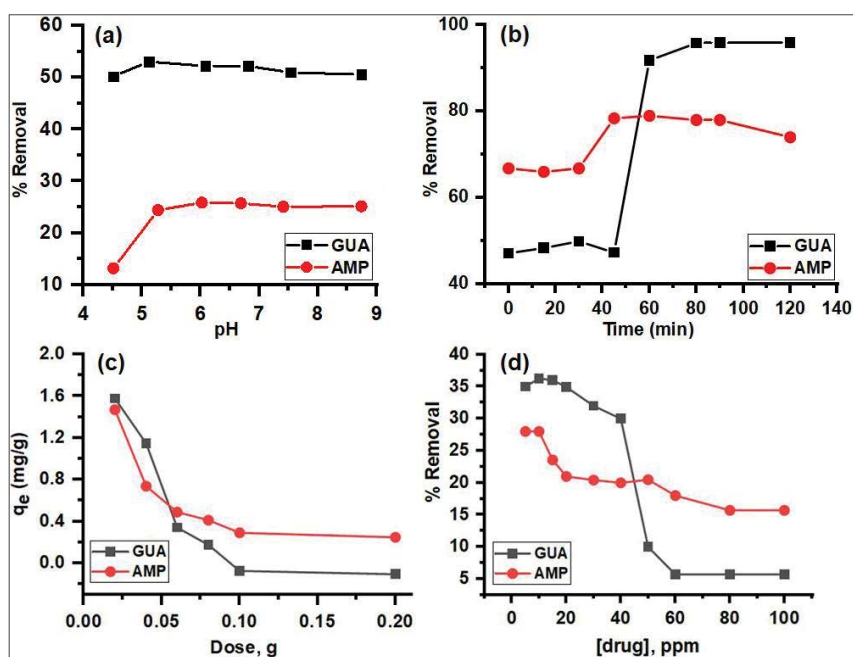


Fig. 4. Effect of: (a) pH, (b) shaking time, (c) sorbent dose, and (d) initial drug concentration on the removal of guaifenesin and amprolium drugs by chitosan sorbent.

*3.4. Effect of sorbent dose on the sorption capacity*

The effect of sorbent dose was studied using a variable amount in the range of 0.02–0.2 g and keeping all other parameters constant. Both drugs have demonstrated similar results as shown in Fig. 4c. The ability to adsorb drugs has decreased with increasing the adsorbent dose. An amount of 0.02 g of the CS sorbent has given the optimum adsorption capacity, this could be attributed to the overlapping of active sites due to sorbent particles overcrowding [44,45]. In addition, the decrease of the quantity of adsorbed particles per 1.0 g of sorbent ($q_e$) can be attributed to the scattering effect of the diffusion between adsorbates, which contributes to a decrease in the amount of drug adsorbed to the unit mass of the CS sorbent [45].

*3.5. Effect of drug capacity*

Drug capacity have a great impact on the adsorption process. The initial drug concentration effect was investigated using the concentration range of 10–100 ppm and the results are represented in Fig. 4d. The results show a decrease in the removal percentage with increasing drug concentration. The maximum removal percentage was found to be 36% and 28% for GUA and AMP, respectively, at a drug concentration of 10 ppm. The explanations for such behavior might be due to the increased mobility of drug particles in dilute solutions, leading increased interaction between adsorbed particles and the adsorbent [46]. Another explanation for these results is the accessibility of adsorption sites on the adsorbent surface. When the drug concentration is low, there will be available adequate adsorption sites for drug molecules, while at higher concentrations, the available active sites are limited and would have become saturated which induces a decrease in removal [47,48]. Even though, the removal percentage of the drugs decreases as the initial drug concentration increases, the adsorption capacity ($q_e$) increased as represented in Fig. 5. It may be ascribed to the fact that as the drug concentration increases; the diffusion resistance decreases and the probability of collision among the adsorbate molecules and adsorbent surface increases, which resulted in the usage of the most active sites available for adsorption, indicating a greater adsorption capacity [49–51].

*3.6. Adsorption isotherm*

Adsorption isotherm models of Langmuir and Freundlich were applied to assess the efficiency of chitosan for the removal of GUA and AMP drugs. Langmuir isotherm shows that the surface of sorbent is homogenous, and the sorption process took place as a monolayer adsorption. Eq. (3) represents the linear form of Langmuir model [52,53]:

$$\frac{C_e}{q_e} = \frac{1}{q_m}C_e + \frac{1}{q_m K_L} \tag{3}$$

where $q_m$ (mg/g), $K_L$ (L/mg) is the maximum adsorption capacity, and Langmuir constant, respectively [54].

Fig. 6a shows the linear fitting for the plot of $C_e/q_e$ against $C_e$, the Langmuir parameters and the correlation coefficient are listed in Table 1.

The Freundlich isotherm assumes that the interaction between liquid and solid phase depends on multilayer adsorption, that is, heterogeneous surface. Eq. (4) represents the linear form of Freundlich isotherm model:
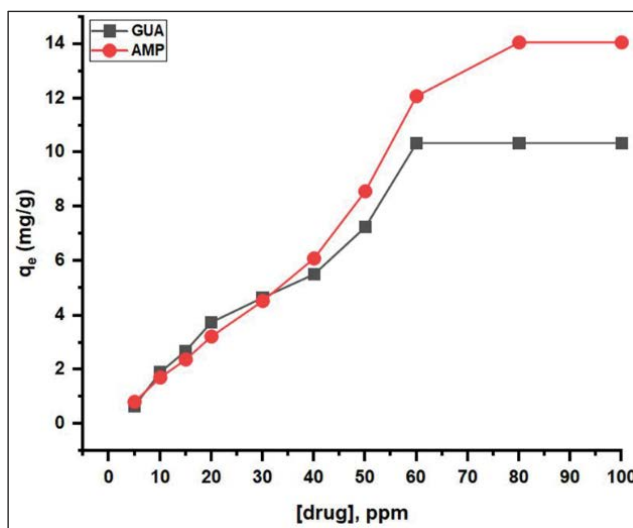


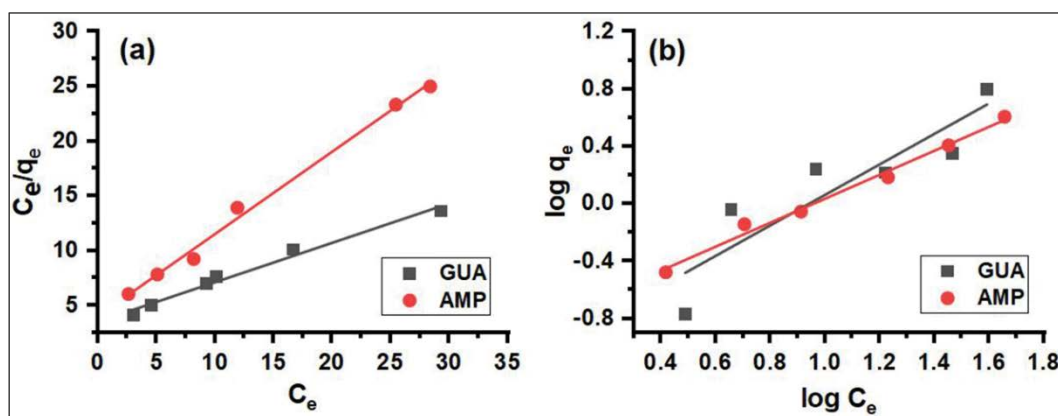Fig. 5. Effect of the drugs initial concentration on the adsorption capacity.



Fig. 6. Adsorption isotherm models for the removal of guaifenesin and amprolium by chitosan: (a) Langmuir and (b) Freundlich model.

$$\log q_e = \log K_f + \frac{1}{n}\log C_e \qquad (4)$$

where $K_f$ (mg/g) and ($n$) refer to Freundlich constant and Freundlich exponent, respectively as ($n$) describes the relative distribution of energy and the heterogeneous nature of adsorbent surface. $K_f$ and $1/n$ values were estimated from the plot of $\log(q_e)$ against $\log(C_e)$ in Fig. 6b with the respective correlation coefficient listed in Table 1. Langmuir model gives the best fitting correlation to the experimental data. It can be observed from the results that Langmuir isotherm is able to describe the adsorption process more than Freundlich with correlation coefficient $R^2 = 0.984$, $0.994$ and the $q_m$ is 2.78, 1.33 for GUA and AMP, respectively. The magnitude of the exponent $1/n$ gives an indication of the favorability of adsorption. The value of $n > 1$ represents favorable adsorption condition. The value of $1/n$ within the range of 1–10 confirms the favorable condition for adsorption. These results infer that the adsorption process of both drugs may be described as a monolayer adsorption on chitosan surface [55].

### 3.7. Kinetics studies

To analyze the adsorption mechanism of the uptake of GUA and AMP by CS sorbent, the experimental results were evaluated using pseudo-first-order, pseudo-second-order, Elovich, and intraparticle diffusion kinetic models.

#### 3.7.1. Pseudo-first-order and pseudo-second-order kinetic models

The pseudo-first-order and pseudo-second-order kinetic models can be represented by Eqs. (5) and (6), respectively [56,57]:

$$\log\left(q_e - q_t\right) = \log q_e - \frac{k_1}{2.303}t \qquad (5)$$

$$\frac{t}{q_t} = \frac{1}{\left(k_2 q_e^2\right)} + \frac{t}{q_e} \qquad (6)$$

where $q_e$ and $q_t$ are the amount of adsorbed particles per 1.0 g of chitosan (mg/g) at equilibrium and at any time $t$, respectively, $k_1$ (min$^{-1}$) and $k_2$ (g/mg min) are the rate constants for pseudo-first-order and pseudo-second-order reactions, respectively. Fig. 7a and b show the linear fit of the experimental data to Eqs. (5) and (6), respectively, and the slope and intercept were used to calculate the kinetic parameters for GUA and AMP and are listed in Table 2 with their corresponding correlation coefficients ($R^2$).

From these results, and based on the value of correlation coefficient ($R^2 > 0.99$) for GUA drug, the adsorption process can be interpreted by pseudo-second-order kinetic model rather than pseudo-second-order model, suggesting that the rate-determining step depends on the concentrations of both adsorbate and adsorbent [59], which means that chemical adsorption was the rate-limiting step of the adsorption mechanism [60].

As for AMP drug, although the $R^2$ is significantly high for pseudo-first-order model (0.962), its value still higher for the pseudo-second-order model (0.992), which makes the later a suggested model for the adsorption of AMP on CS, meaning that chemical adsorption is most probably the rate-limiting step of the adsorption process [60].

#### 3.7.2. Elovich kinetic model

The Elovich kinetic models is usually applied for studying of chemisorption on highly heterogeneous adsorbents,

Table 1
Langmuir and Freundlich parameters for guaifenesin and amprolium removal by chitosan

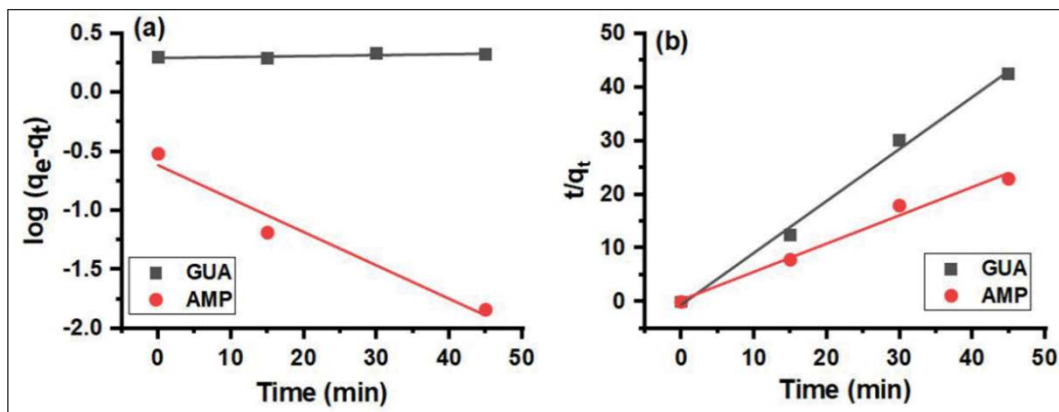| Drugs | Langmuir model | | | Freundlich model | | |
|---|---|---|---|---|---|---|
| | $q_m$ (mg/g) | $K_L$ (L/mg) | $R^2$ | $K_f$ | $n$ | $R^2$ |
| Guaifenesin | 2.78 | 0.100 | 0.984 | 0.100 | 1.06 | 0.811 |
| Amprolium | 1.33 | 0.186 | 0.994 | 0.159 | 0.835 | 0.987 |



Fig. 7. (a) Pseudo-first-order and (b) pseudo-second-order kinetic models for removal of guaifenesin and amprolium by chitosan.

it's based on the Elovich Eq. (7). It describes the process of chemisorption of sorbates molecules on a solid surface without desorption of the substance, the rates may decrease with time due to an increase in surface coverage [61]:

$$q_t = \frac{1}{\beta}\ln(\alpha\beta) + \frac{1}{\beta}\ln t \tag{7}$$

where $\alpha$ is the initial adsorption rate (mg/g·min) and $\beta$ is the desorption constant (g/mg). The parameters of the Elovich equation are summarized in Table 2. The Elovich kinetic model for the adsorption of both drugs by CS is represented in Fig. 8.

This kinetic model also explain that the adsorption process could probably be chemisorption corresponding to the heterogeneous nature of the active sites. $R^2$ value of GUA = 0.609 and for AMP = 0.865, these values are relatively

lower than the values obtained from pseudo-second-order kinetic model.

### 3.7.3. Intraparticle diffusion kinetic model

The intraparticle diffusion kinetic model can be represented by Eq. (8) [62]:

$$q_t = K_p t^{1/2} + C \tag{8}$$

where $p$ is intraparticle diffusion rate constant (mg/g·min$^{-1/2}$) and $C$ is intercept of the plot, $K$ indicates the boundary layer effect. The linear regression plots of $t$ vs. $t^{1/2}$ is obtained under the optimum condition for drugs sorption onto CS. The deviation from the origin in Fig. 9 reveals the existence of some boundary layer effect.

Table 2
Summary of the kinetic parameters and $R^2$ values of pseudo-first-order, pseudo-second-order, Elovich, and intraparticle diffusion models interpreted for adsorption of guaifenesin and amprolium by chitosan

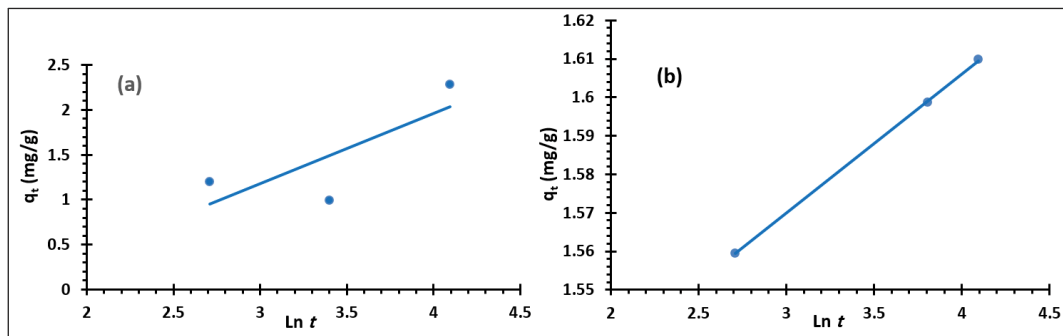| Drugs | Pseudo-first-order | | | Pseudo-second-order | | | Elovich model | | | Intraparticle diffusion | | |
|---|---|---|---|---|---|---|---|---|---|---|---|---|
| | $q_e$ (mg/g) | $k_1$ (min$^{-1}$) | $R^2$ | $q_e$ (mg/g) | $k_2$ (g/mg·min) | $R^2$ | $\alpha$ (mg/g·min) | $\beta$ (g/mg) | $R^2$ | $K^{0.5}$ (mg/g·min$^{0.5}$) | $C$ | $R^2$ |
| Guaifenesin | 1.97 | $1.86 \times 10^{-3}$ | 0.555 | 1.032 | 0.57 | 0.995 | 0.018 | 1.277 | 0.609 | 0.085 | 0.447 | 0.938 |
| Amprolium | 0.94 | 0.53 | 0.962 | 1.898 | 1.25 | 0.992 | $1.9 \times 10^{15}$ | 8.4 | 0.865 | 0.134 | 0.588 | 0.944 |



Fig. 8. Elovich kinetic model for the adsorption of (a) guaifenesin and (b) amprolium drugs by chitosan.
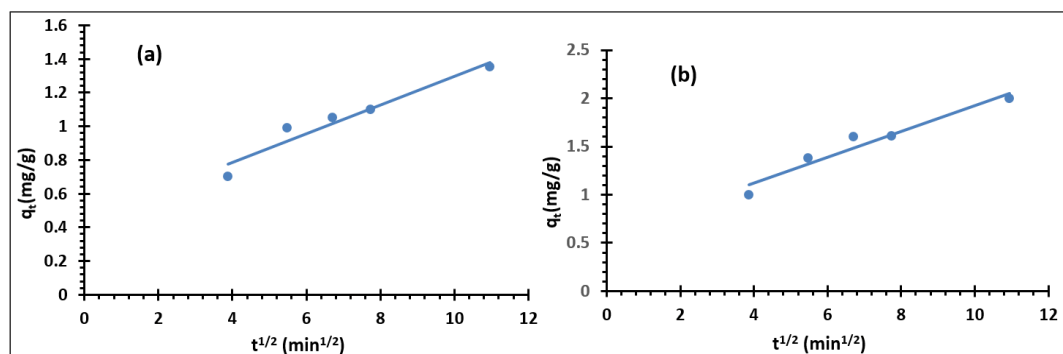


Fig. 9. Intraparticle diffusion model fitted to the adsorption data of for the adsorption of (a) guaifenesin and (b) amprolium drugs by chitosan.

Table 2 shows the intraparticle diffusion parameters for adsorption. Although the $R^2$ value for intraparticle diffusion model are significantly high for both drugs (0.938 and 0.944 for GUA and AMP drugs, respectively); it's still lower than the $R^2$ values for pseudo-second-order (0.995 and 0.992 for GUA and AMP drugs, respectively) which means that the adsorption is not intraparticle diffusion-controlled.

### 3.8. Thermodynamics studies

Gibbs equation and the Van't Hoff equation are used to evaluate thermodynamic parameters, such as Gibbs free energy ($\Delta G°$), entropy ($\Delta S°$), and enthalpy ($\Delta H°$), were evaluated using Eqs. (9)–(11). The values of these parameters are listed in Table 3:

$$\Delta G° = -RT \ln K_c \tag{9}$$

$$\ln K_c = \frac{\Delta S°}{R} - \frac{\Delta H°}{RT} \tag{10}$$

$$\Delta G° = \Delta H° - T\Delta S° \tag{11}$$

where $R$ represents the universal gas constant ($8.3145 \times 10^{-3}$ kJ/mol·K), $K_c$ ($C_{ad}/C_e$) represents the distribution coefficient for the sorption, $C_{ad}$ (mg/L) is the amount of drug adsorbed on the sorbent at equilibrium, and $T$ is the temperature in K.

A plot of straight line has been obtained (as shown in Fig. 10) representing the relation between $\ln K_c$ and $1/T$.

The positive values of $\Delta G°$ reflect the nonspontaneous nature of this adsorption process. The positive values of $\Delta H°$ indicate that the adsorption process was endothermic process and positive value of $\Delta S°$ implied the increasing randomness at the solid surface during the adsorption of the drugs on CS ($\Delta S° > 0$ for spontaneous process) [63,64].

Table 4
Comparison of the removal efficiency of guaifenesin and amprolium by chitosan with other adsorbents

| Drugs | Adsorbent materials | Removal efficiency | References |
|---|---|---|---|
| Guaifenesin | Activated charcoal | 60% | [58] |
| Amprolium | *Salvadora persica* roots ash | 98% | [59] |
| | *Salvadora persica* seeds ash | 96% | |
| Guaifenesin | Chitosan | 95% | This work |
| Amprolium | Chitosan | 79% | This work |

Table 3
Thermodynamics of the sorption of amprolium and guaifenesin onto chitosan

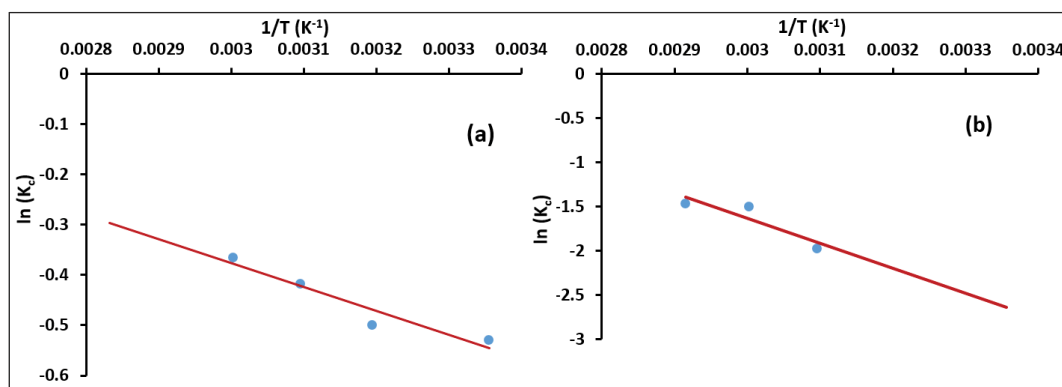| Drug | Temperature (K) | $K_d$ | Gibbs free energy $\Delta G°$ (kJ/mol) | Enthalpy $\Delta H°$ (kJ/mol) | Entropy $\Delta S°$ (J/K·mol) | Activation energy $E_a$ (kJ/mol) |
|---|---|---|---|---|---|---|
| Amprolium | 298 | 0.589 | 1.323 | | | 6.358 |
| | 313 | 0.606 | 1.195 | | | 6.482 |
| | 323 | 0.658 | 1.109 | 3.879 | 0.009 | 6.566 |
| | 333 | 0.693 | 1.023 | | | 6.649 |
| | 353 | 0.658 | 0.852 | | | 6.815 |
| Guaifenesin | 298 | 1.626 | 6.542 | | | 25.969 |
| | 303 | 0.455 | 6.258 | | | 26.010 |
| | 323 | 0.139 | 5.120 | 23.491 | 0.057 | 26.177 |
| | 333 | 0.022 | 4.552 | | | 26.259 |
| | 343 | 0.229 | 3.983 | | | 26.343 |



Fig. 10. A thermodynamic plot of $\ln K_c$ against $1/T$ for sorption of (a) amprolium and (b) guaifenesin onto chitosan sorbent.

## 3.9. Comparison with other adsorbents

Table 4 compares the efficacy of chitosan and other adsorbents for the elimination of GUA and AMP from aqueous medium. Abdulkhair et al. [65] applied activated carbon for the removal of GUA with removal percentage of 60%, and Ali et al. [66] employed roots and seeds ash of *Salvadora persica* for the removal of AMP with removal percentage of 98% and 96%, respectively. It could be inferred that the adsorption capacity of chitosan is comparable with other adsorbents for both GUA and AMP.

## 4. Conclusion

The uptake of guaifenesin (GUA) and amprolium (AMP) onto chitosan (CS) biosorbent was investigated. The influence of various factors on the adsorption process such as solution pH, time, adsorbent dose and drug capacity were examined. The optimum conditions were pH 6.0, shaking time of 60 min for both drugs. The best sorbent amount and the drug capacity for both drugs were found to be 0.02 g and 10 ppm, respectively. The experimental data were described well with Langmuir isotherm model for both drugs. The thermodynamic study showed that the process is highly endothermic in nature, with positive values of Gibbs free energy, enthalpy and changes in the entropy. Furthermore, the adsorption mechanism obeys pseudo-second-order kinetic model. Chitosan has a significant removal capability for (GUA) and (AMP) drugs from wastewater of 95% and 79%, respectively.

## Disclosure statement

- Competing interests: all authors participating in this work declare that no conflict of interest exists.
- Ethics approval and consent to participate: this work does not contain any studies with human or animal participants.
- Consent for publication: all authors have agreed to publish this work.
- Availability of data and material: data and materials used/produced by this work are available and/or reproducible.
- Funding: This work was funded by the Deputyship for Research & Innovation, Ministry of Education in Saudi Arabia, project number 442/16.

## References

[1] L. Chen, X. Zhang, Y. Xu, X. Du, X. Sun, L. Sun, H. Wang, Q. Zhao, A. Yu, H. Zhang, L. Ding, Determination of fluoroquinolone antibiotics in environmental water samples based on magnetic molecularly imprinted polymer extraction followed by liquid chromatography-tandem mass spectrometry, Anal. Chim. Acta, 662 (2010) 31–38.

[2] C. Avila, J. Nivala, L. Olsson, K. Kassa, T. Headley, R.A. Mueller, J.M. Bayona, J. Garcia, Emerging organic contaminants in vertical subsurface flow constructed wetlands: influence of media size, loading frequency and use of active aeration, Sci. Total Environ., 494–495 (2014) 211–217.

[3] C. Yan, Y. Yang, J. Zhou, M. Nie, M. Liu, M.F. Hochella Jr., Selected emerging organic contaminants in the Yangtze Estuary, China: a comprehensive treatment of their association with aquatic colloids, J. Hazard. Mater., 283 (2015) 14–23.

[4] K.M. Kasiotis, C. Emmanouil, P. Anastasiadou, A. Papadi-Psyllou, A. Papadopoulos, O. Okay, K. Machera, Organic pollution and its effects in the marine mussel *Mytilus galloprovincialis* in Eastern Mediterranean coasts, Chemosphere, 119 (2015) S145–152.

[5] H.H. Albrecht, P.V. Dicpinigaitis, E.P. Guenin, Role of guaifenesin in the management of chronic bronchitis and upper respiratory tract infections, Multidiscip. Respir. Med., 12 (2017) 1–11.

[6] E. Temmel, M.J. Eicke, F. Cascella, A. Seidel-Morgenstern, H. Lorenz, Resolution of racemic guaifenesin applying a coupled preferential crystallization-selective dissolution process: rational process development, Cryst. Growth Des., 19 (2019) 3148–3157.

[7] M.R. Elamin, A.O. Elzupir, B.Y. Abdulkhair, Synthesis and characterization of functionalized carbon nanofibers for efficient removal of highly water-soluble dextromethorphan and guaifenesin from environmental water samples, Environ. Nanotechnol. Monit. Manage., 15 (2021) 100397, doi: 10.1016/j.enmm.2020.100397.

[8] M.A. Basha, M.K. Abd El-Rahman, L.I. Bebawy, A.A. Moustafa, S.A. Hassan, A comparative study of two analytical techniques for the simultaneous determination of amprolium HCl and ethopabate from combined dosage form and in presence of their alkaline degradation, Spectrochim. Acta, Part A, 243 (2020) 118756, doi: 10.1016/j.saa.2020.118756.

[9] M. Ali, N. Chand, R.U. Khan, S. Naz, S. Gul, Anticoccidial effect of garlic (*Allium sativum*) and ginger (*Zingiber officinale*) against experimentally induced coccidiosis in broiler chickens, J. Appl. Anim. Res., 47 (2019) 79–84.

[10] A. De Lahunta, E.N. Glass, M. Kent, Veterinary Neuroanatomy and Clinical Neurology-e-Book, Elsevier Health Sciences, 2014.

[11] D.W. Duszynski, J. Kvičerová, R.S. Seville, Treatment and Drug Therapies of Coccidiosis in Carnivora, D.W. Duszynski, J. Kvičerová, R.S. Seville, Eds., The Biology and Identification of the Coccidia (Apicomplexa) of Carnivores of the World, Academic Press, Cambridge, Massachusetts, United States, 2018, pp. 445–463.

[12] A.B.A. Boxall, D.W. Kolpin, B. Halling-Sorensen, J. Tolls, Are veterinary medicines causing environmental risks?, Environ. Sci. Technol., 37 (2003) 286A–294A.

[13] S. Bergeron, R. Boopathy, R. Nathaniel, A. Corbin, G. LaFleur, Presence of antibiotic resistant bacteria and antibiotic resistance genes in raw source water and treated drinking water, Int. Biodeterior. Biodegrad., 102 (2015) 370–374.

[14] O. Bansal, Antibiotics in hospital effluents and their impact on the antibiotics resistant bacteria and remediation of the antibiotics: a review, Network Pharmacol., 4 (2019) 6–30.

[15] A. Rodayan, P.A. Segura, V. Yargeau, Ozonation of wastewater: removal and transformation products of drugs of abuse, Sci. Total Environ., 487 (2014) 763–770.

[16] B. Ensano, L. Borea, V. Naddeo, V. Belgiorno, M. de Luna, F. Ballesteros, Removal of pharmaceuticals from wastewater by intermittent electrocoagulation, Water, 9 (2017) 85–99.

[17] C.M. Lopez-Ortiz, I. Sentana-Gadea, P.J. Varo-Galvan, S.E. Maestre-Perez, D. Prats-Rico, Effect of magnetic ion exchange (MIEX®) on removal of emerging organic contaminants, Chemosphere, 208 (2018) 433–440.

[18] G.F. da Silva Brito, R. Oliveira, C.K. Grisolia, L.S. Guirra, I.T. Weber, F.V. de Almeida, Evaluation of advanced oxidative

processes in biodiesel wastewater treatment, J. Photochem. Photobiol., A, 375 (2019) 85–90.

[19] M. Verma, A.K. Haritash, Degradation of amoxicillin by Fenton and Fenton-integrated hybrid oxidation processes, J. Environ. Chem. Eng., 7 (2019) 102886, doi: 10.1016/j.jece.2019.102886.

[20] B. Radel, M. Funck, T.H. Nguyen, H. Nirschl, Determination of filtration and consolidation properties of protein crystal suspensions using analytical photocentrifuges with low volume samples, Chem. Eng. Sci., 196 (2019) 72–81.

[21] S. Praveen, J. Jegan, T. Bhagavathi Pushpa, R. Gokulan, L. Bulgariu, Biochar for removal of dyes in contaminated water: an overview, Biochar, 4 (2022) 10.

[22] T. Adachi, E. Isobe, Fundamental characteristics of synthetic adsorbents intended for industrial chromatographic separations, J. Chromatogr. A, 1036 (2004) 33–44.

[23] M. Ghaedi, A.G. Nasab, S. Khodadoust, M. Rajabi, S. Azizian, Application of activated carbon as adsorbents for efficient removal of methylene blue: kinetics and equilibrium study, J. Ind. Eng. Chem., 20 (2014) 2317–2324.

[24] M.H. Al-Malack, A.A. Basaleh, Adsorption of heavy metals using activated carbon produced from municipal organic solid waste, Desal. Water Treat., 57 (2016) 24519–24531.

[25] M.K. Uddin, A review on the adsorption of heavy metals by clay minerals, with special focus on the past decade, Chem. Eng. J., 308 (2017) 438–462.

[26] A.E.S. Choi, S. Roces, N. Dugos, A. Arcega, M.-W. Wan, Adsorptive removal of dibenzothiophene sulfone from fuel oil using clay material adsorbents, J. Cleaner Prod., 161 (2017) 267–276.

[27] Y. Dai, Q. Sun, W. Wang, L. Lu, M. Liu, J. Li, S. Yang, Y. Sun, K. Zhang, J. Xu, W. Zheng, Z. Hu, Y. Yang, Y. Gao, Y. Chen, X. Zhang, F. Gao, Y. Zhang, Utilizations of agricultural waste as adsorbent for the removal of contaminants: a review, Chemosphere, 211 (2018) 235–253.

[28] S.M. Nomanbhay, K. Palanisamy, Removal of heavy metal from industrial wastewater using chitosan coated oil palm shell charcoal, Electronic J. Biotechnol., 8 (2005) 43–53.

[29] X. Wang, Y. Du, L. Fan, H. Liu, Y. Hu, Chitosan-metal complexes as antimicrobial agent: synthesis, characterization and structure-activity study, Polym. Bull., 55 (2005) 105–113.

[30] T.K. Saha, N.C. Bhoumik, S. Karmaker, M.G. Ahmed, H. Ichikawa, Y. Fukumori, Adsorption of methyl orange onto chitosan from aqueous solution, J. Water Resour. Prot., 2 (2010) 898–906.

[31] N.B. Singh, G. Nagpal, S. Agrawal, Rachna, water purification by using adsorbents: a review, Environ. Technol. Innovation, 11 (2018) 187–240.

[32] M. Yousefi, E. Jabbari, M. Sedighi, Experimental study of polyaluminum chloride-chitosan coagulant for water treatment using response surface methodology, J. Appl. Res. Water Wastewater, 9 (2022) 23–29.

[33] D. Senol-Arslan, Isotherms, kinetics and thermodynamics of Pb(II) adsorption by crosslinked chitosan/sepiolite composite, Polym. Bull., 79 (2022) 3911–3928.

[34] S.M. Sirry, F. Aldakhil, O.M.L. Alharbi, I. Ali, Chemically treated date stones for uranium(VI) uptake and extraction in aqueous solutions, J. Mol. Liq., 273 (2019) 192–202.

[35] S. Ali, S.M. Sirry, H.A. Hassanin, Removal and characterisation of Pb(II) ions by xylenol orange-loaded chitosan: equilibrium studies, Int. J. Environ. Anal. Chem., 102 (2022) 6257–6269.

[36] A. Li, R. Lin, C. Lin, B. He, T. Zheng, L. Lu, Y. Cao, An environment-friendly and multi-functional absorbent from chitosan for organic pollutants and heavy metal ion, Carbohydr. Polym., 148 (2016) 272–280.

[37] R. Varma, S. Vasudevan, Extraction, characterization, and antimicrobial activity of chitosan from horse mussel *modiolus*, ACS Omega, 5 (2020) 20224–20230.

[38] J. Carneiro, P.M. Döll-Boscardin, B.C. Fiorin, J.M. Nadal, P.V. Farago, J.P. de Paula, Development and characterization of hyaluronic acid-lysine nanoparticles with potential as innovative dermal filling, Braz. J. Pharm. Sci., 52 (2016) 645–651.

[39] A.M. Thawabteh, Synthesis and Characterization of Designed Guaifenesin Prodrugs, M. Sc. Thesis, Deanship of Graduate Studies Al-Quds University, Jerusalem, Palestine, 2015.

[40] S. Kumar, J. Koh, Physiochemical, optical and biological activity of chitosan-chromone derivative for biomedical applications, Int. J. Mol. Sci., 13 (2012) 6102–6116.

[41] P. Acharya, T. Prasanth Kumar, I. Agasteen, S. Rajasekhar, G. Neelima, M.G. Neelima, A review on analytical methods for determination of guaifenesin alone and in combination with other drugs in pharmaceutical formulations, Saudi J. Med. Pharm. Sci., 3 (2017) 148–159.

[42] M.A. Basha, M.K. Abd El-Rahman, L.I. Bebawy, M.Y. Salem, Novel potentiometric application for the determination of amprolium HCl in its single and combined dosage form and in chicken liver, Chin. Chem. Lett., 28 (2017) 612–618.

[43] M. Sarma, T. Chatterjee, S.K. Das, Ammonium–crown ether based host–guest systems: N–H···O hydrogen bond directed guest inclusion featuring N–H donor functionalities in angular geometry, RSC Adv., 2 (2012) 3920–3926.

[44] H. Lata, S. Mor, V.K. Garg, R.K. Gupta, Removal of a dye from simulated wastewater by adsorption using treated parthenium biomass, J. Hazard. Mater., 153 (2008) 213–220.

[45] N. Delaila Tumin, A.L. Chuah, Z. Zawani, S.A. Rashid, Adsorption of copper from aqueous solution by *Elais guineensis* kernel activated carbon, J. Eng. Sci. Technol., 3 (2008) 180–189.

[46] A.A. Morsy, H. Kamal, N. Walley, M. Rageh, M. Badewy, Uranium removal from its liquid waste using chemically treated rice husk, J. Earth Environ. Health Sci., 2 (2016) 41–49.

[47] B.V. Babu, S. Gupta, Adsorption of Cr(VI) using activated neem leaves: kinetic studies, Adsorption, 14 (2007) 85–92.

[48] E. Suganya, N. Saranya, C. Patra, L.A. Varghese, N. Selvaraju, Biosorption potential of *Gliricidia sepium* leaf powder to sequester hexavalent chromium from synthetic aqueous solution, J. Environ. Chem. Eng., 7 (2019) 103112, doi: 10.1016/j.jece.2019.103112.

[49] H. Faghihian, S. Peyvandi, Adsorption isotherm for uranyl biosorption by *Saccharomyces cerevisiae* biomass, J. Radioanal. Nucl. Chem., 293 (2012) 463–468.

[50] G. Karayel Incili, G.A. Aycık, Chemical modification of silica gel with synthesized Schiff base hydrazone derivative and application for preconcentration and separation of U(VI) ions from aqueous solutions, J. Radioanal. Nucl. Chem., 301 (2014) 417–426.

[51] L. Li, N. Hu, D. Ding, X. Xin, Y. Wang, J. Xue, H. Zhang, Y. Tan, Adsorption and recovery of U(VI) from low concentration uranium solution by amidoxime modified *Aspergillus niger*, RSC Adv., 5 (2015) 65827–65839.

[52] I. Langmuir, The adsorption of gases on plane surfaces of glass, mica and platinum, J. Am. Chem. Soc., 40 (2002) 1361–1403.

[53] K. Zhou, Y. Liu, Z. Yang, H. Liu, Biosorption of U(VI) by modified Hottentot Fern: kinetics and equilibrium studies, J. Environ. Radioact., 167 (2017) 13–19.

[54] R.M. Ali, H.A. Hamad, M.M. Hussein, G.F. Malash, Potential of using green adsorbent of heavy metal removal from aqueous solutions: adsorption kinetics, isotherm, thermodynamic, mechanism and economic analysis, Ecol. Eng., 91 (2016) 317–332.

[55] M. Ahmad, A.R.A. Usman, S.S. Lee, S.-C. Kim, J.-H. Joo, J.E. Yang, Y.S. Ok, Eggshell and coral wastes as low-cost sorbents for the removal of $Pb^{2+}$, $Cd^{2+}$ and $Cu^{2+}$ from aqueous solutions, J. Ind. Eng. Chem., 18 (2012) 198–204.

[56] M. Monier, D.M. Ayad, Y. Wei, A.A. Sarhan, Adsorption of Cu(II), Co(II), and Ni(II) ions by modified magnetic chitosan chelating resin, J. Hazard. Mater., 177 (2010) 962–970.

[57] A. Naga Babu, G.V. Krishna Mohan, K. Kalpana, K. Ravindhranath, Removal of lead from water using calcium alginate beads doped with hydrazine sulphate-activated red mud as adsorbent, J. Anal. Methods Chem., 2017 (2017) 1–13.

[58] G. Crini, P.-M. Badot, Application of chitosan, a natural aminopolysaccharide, for dye removal from aqueous solutions by adsorption processes using batch studies: a review of recent literature, Prog. Polym. Sci., 33 (2008) 399–447.

[59] Y.S. Ho, G. McKay, A comparison of chemisorption kinetic models applied to pollutant removal on various sorbents, Process Saf. Environ. Prot., 76 (1998) 332–340.

[60] Y. Zhou, S. Fu, L. Zhang, H. Zhan, M.V. Levit, Use of carboxylated cellulose nanofibrils-filled magnetic chitosan hydrogel beads as adsorbents for Pb(II), Carbohydr. Polym., 101 (2014) 75–82.

[61] I. Ismi, H. Elaidi, A. Ouass, L. Chafki, H. Essebaai, H. Bousfiha, A. Lebkiri, E.H. Rifi, Kinetic analysis and isotherm modeling for the adsorption of silver ion from aqueous solution on a superabsorbent polymer, J. Mater. Environ. Sci., 8 (2017) 4705–4715.

[62] S. Agarry, O. Ogunleye, O. Ajani, Biosorptive removal of cadmium(II) ions from aqueous solution by chemically modified onion skin: batch equilibrium, kinetic and thermodynamic studies, Chem. Eng. Commun., 202 (2015) 655–673.

[63] E. Moawed, N. Burham, M. El-Shahat, Selective separation and determination of copper and gold in gold alloy using ion exchange polyurethane foam, J. Liq. Chromatogr. Relat. Technol., 30 (2007) 1903–1914.

[64] O. Adam, Removal of resorcinol from aqueous solution by activated carbon: isotherms, thermodynamics and kinetics, Am. Chem. Sci. J., 16 (2016) 1–13.

[65] B.Y. Abdulkhair, M.R. Elamin, A.O. Elzupir, Comprehension to dextromethorphan and guaifenesin antibiotics adsorption on activated charcoal from water: kinetics, thermodynamics, and solution parameters, J. Optoelectron. Biomed. Mater., 11 (2019) 19–27.

[66] S. Ali, A. Abdelhalim, Removal of amprolium from water by roots and seeds ash of *Salvadora persica*, J. Taibah Univ. Sci., 14 (2020) 1604–1612.